

Dynamics of laminar magnetic vortex rings

T. Roesgen and M. Gharib

Citation: *Phys. Fluids A* **5**, 515 (1993); doi: 10.1063/1.858878

View online: <http://dx.doi.org/10.1063/1.858878>

View Table of Contents: <http://pof.aip.org/resource/1/PFADEB/v5/i2>

Published by the AIP Publishing LLC.

Additional information on Phys. Fluids A

Journal Homepage: <http://pof.aip.org/>

Journal Information: http://pof.aip.org/about/about_the_journal

Top downloads: http://pof.aip.org/features/most_downloaded

Information for Authors: <http://pof.aip.org/authors>

ADVERTISEMENT

The logo for AIP Advances, featuring the word 'AIP' in a large, bold, blue font, followed by the word 'Advances' in a smaller, green font. Above the text is a decorative graphic of several orange circles of varying sizes, some connected by a dotted line, suggesting a path or a sequence of events.

Submit Now

**Explore AIP's new
open-access journal**

- **Article-level metrics
now available**
- **Join the conversation!
Rate & comment on articles**

Dynamics of laminar magnetic vortex rings

T. Roesgen^{a)}
 IRS, Stuttgart University, Germany

M. Gharib
 AMES Department, University of California, San Diego, La Jolla, California 92093

(Received 23 June 1992; accepted 1 October 1992)

Preliminary results are reported for an experiment studying the dynamics of laminar magnetic vortex rings. These are formed through injection of a magnetic fluid (ferrofluid) into a nonmagnetic carrier liquid. An external magnetic field is used to strain the magnetic cores of the propagating rings without an additional external flow and away from solid boundaries. Varying field-dependent growth rates and the development of field-induced instabilities can be observed. Results are presented from an automated analysis of digitally recorded video sequences, resulting in time records of the evolving ring radii.

Ferrofluids are suspensions of small ferromagnetic particles in an inert carrier liquid. Through the use of very small particles (~ 10 nm) and special surfactant coatings, coagulation and settling effects are eliminated and a fluid is created with long-term stability and essentially Newtonian behavior in the field-free case. In the case of nonzero external magnetic fields, ferrofluids show a magnetization curve without hysteresis ("superparamagnetism") and feature both additional internal forces and an increasingly anisotropic viscosity. The concept underlying this investigation is the use of these field-induced effects for control and manipulation of large coherent structures in an otherwise "conventional" flow. The propagation of laminar vortex rings proves to be particularly well suited due to the simple topologies involved. While the generation of instabilities on the rings could be observed already for static magnetic fields, it is anticipated that dynamic forcing or spatial modulation of the force field in the azimuthal direction may provide much more flexible tools to study vortex dynamics.

Following the theory as presented by Rosensweig,¹ an additional force term has to be included in the Navier-Stokes equations to model the dynamics of magnetic liquids,

$$\mathbf{f}_m = \mu_0 M \nabla H - \nabla \left[\mu_0 \int_0^H \left[-\rho \left(\frac{\partial M}{\partial \rho} \right)_{H,T} + M \right] dH \right],$$

where H denotes the external magnetic field, M the resulting (collinear) magnetization of the fluid, μ_0 the free space permeability, and ρ the fluid density. The first term reflects the dipolar interaction between the fluid particles and the external field. The second one describes an additional pressure contribution which is linked to spatial variations of the magnetization, both due to density dependence and sensitivity to other flow parameters (e.g., temperature).

For isothermal, incompressible flow the terms cancel in the bulk liquid and no net force results. If there are interfaces present between regions of different permeability, however, a force is created at the interface (surface normal \mathbf{n}),

$$\mathbf{f}_m = -\frac{1}{2} H^2 \nabla \mu; \quad \nabla \mu \parallel \mathbf{n}.$$

Here a linear magnetization $M = \chi H$ with a susceptibility $\chi = (\mu/\mu_0 - 1)$ was assumed, implying moderate external magnetic fields. Evaluating the force integral across the interface and applying Green's theorem, a simple expression for the resulting force on an isolated ferrofluid volume can be derived,

$$\begin{aligned} \int_V \mathbf{f}_m dV &= \frac{1}{2} \mu_0 \chi \int_S H^2 \mathbf{n} dA \\ &= \frac{1}{2} \mu_0 \chi \int_V \nabla(H^2) dV \approx \frac{1}{2} \mu_0 \chi V \nabla(H^2), \end{aligned}$$

where the last approximation is valid if the gradient of H^2 is reasonably constant throughout the integration volume.

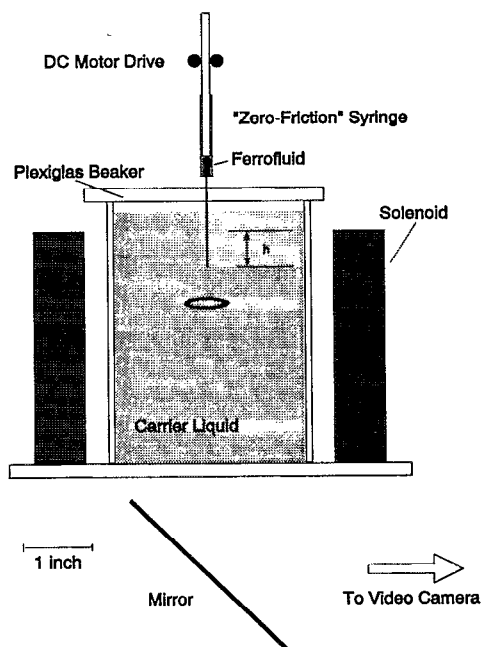


FIG. 1. Experimental setup for the magnetic ring generation.

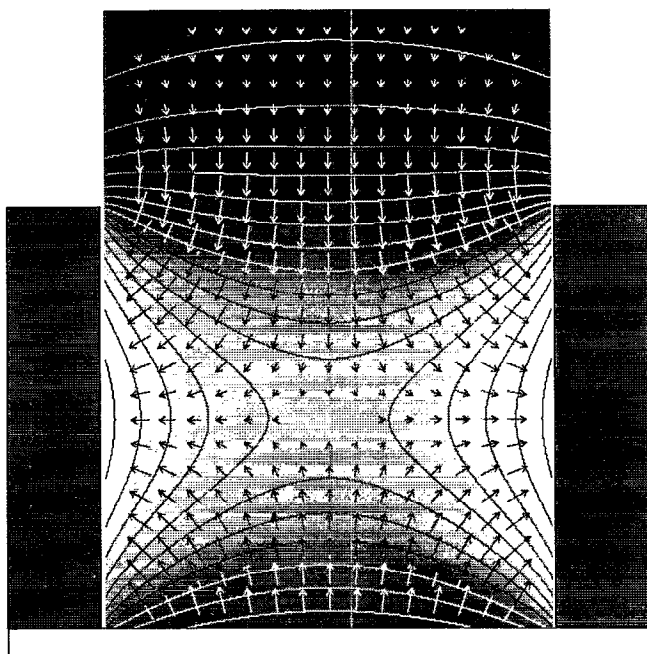


FIG. 2. The magnetic field $|H|^2$ and its gradient inside a cylindrical solenoid.

In a nonhomogeneous liquid, a gradient in the magnetic field consequently does create a net force. The laminar vortex ring with a magnetic core has the required properties of (almost) separable flow regimes and the added advantage that the rotation with its associated pressure gradient tends to preserve the interface even in a destabilizing force field.

For the experiment, a geometry with a high degree of symmetry was chosen (see Fig. 1). The magnetic field is created inside a cylindrical solenoid which surrounds a transparent test chamber, providing a simple way to reach sufficient field strengths. Fig. 2 shows a picture of the magnetic field inside the finite-sized cylindrical solenoid, modeled as a stack of current loops² with the relative dimensions of the actual device. The field squared magnitude H^2 is reflected in the gray level of the picture (bright areas correspond to large values) and the isolines, while the gradient field $\nabla(H^2)$ is indicated by the arrows. Close to the solenoid's exit plane, the forces are predominantly axial and tend to pull in magnetic matter. Approaching the so-

lenoid center, the (relative) radial component of the force vector increases, thus producing a stretching effect. Beyond the solenoid center the sign of the force reverses, creating a local topology similar to a stagnation point flow.

The ferrofluid³ which forms the vortex ring is injected into a lighter, nonmagnetic plenum liquid. In order to achieve density matching, the ferrofluid has to be diluted with its own carrier fluid to a volume fraction φ of about 0.02. Both carrier and plenum liquids are kerosenes with very similar properties, thus minimizing surface tension effects. The vortex ring generator consists of a low friction, seal-free metering syringe, an attached piece of polished steel tubing forming the orifice and a geared dc motor to create a slip-free, programmable electrical drive. Alignment of the ring generator is achieved by monitoring the straightness of the ring trajectories in the axisymmetric magnetic field. The rings are observed in the axial direction through the planar bottom face of the test chamber. A video camera—located a large distance (~ 10 ft) away to avoid parallax effects—is used to record the propagating rings. The video sequences are digitized and processed in digital form.

Rings are generated with constant injection profiles resulting in a Reynolds number of about 50, where $Re = 4V/\pi DT\nu$ is based on the generator's orifice diameter D (8×10^{-4} m), the stroke time T (0.25 sec), the ejected volume V (2.5×10^{-8} m³), and the viscosity ν (3.2×10^{-6} m²/sec). The solenoid (0.092 m i.d., 0.13 m o.d., height 0.089 m) has an equivalent of 38 245 turns/m with a total resistance of 65 Ω . It is operated at four discrete current settings generating field strengths of 0.0, 14.1, 28.2, 42.3 kA/m. In order to create some variability in the force field topology, the rings can be injected at different heights relative to the solenoid's end face ($h = -0.013, 0.0, 0.013$ m, see Fig. 1).

Direct observation of the vortex ring trajectories confirms the expected behavior, that is an increasing amount of stretching with increasing magnetic field. Figure 3 shows the signatures of a magnetic ring injected at $h = 1.27$ cm above the solenoid's rim in a magnetic field of 28.2 kA/m. Four pictures of the same ring were selected at equidistant time intervals (0.5 sec). Following a rapid expansion phase the growth rate is limited at later times. For the parameters chosen, the ring has not (yet) developed any instabilities. Figure 4 compares four *different* rings at the same relative time (1.67 sec) but propagating in dif-

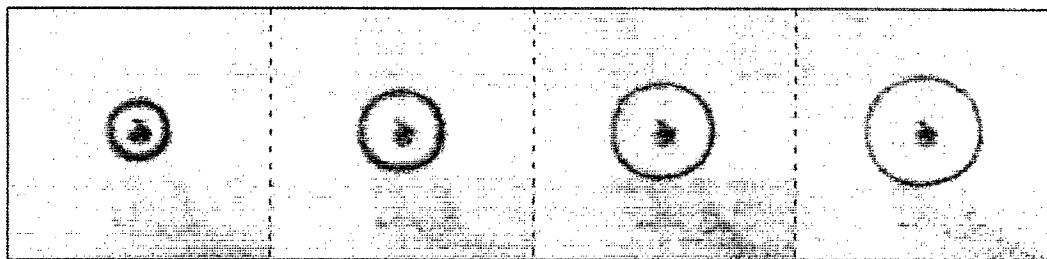


FIG. 3. A vortex ring at different times following injection for an external field of $H = 28.2$ kA/m; (left to right): $t = 0.67, 1.17, 1.67, 2.17$ sec.



FIG. 4. Vortex rings for different magnetic fields at the same time $t=1.67$ sec following injection (left to right): $H=0, 14.1, 28.2, 42.3$ kA/m.

ferent magnetic fields ($\Delta H=14.1$ kA/m). The increasing magnetic forces do not only accelerate the rings' growth but lead to the development of azimuthal instabilities, clearly visible in the last picture. Injection closer to the centerplane of the solenoid results in an almost immediate destruction of the rings when an external field is applied. This is due to the fact that the rings cross the symmetry plane of the magnet in this case and propagate into an adverse force field.

As a first quantitative measurement, the ring diameters were analyzed in the video sequences as a function of time and field strength. The image processing steps included subtraction of a reference image for background elimination, adaptive thresholding to convert the ring signature into a binary image and subsequent measurement of the radius. Figure 5 shows the ring radius as a function of time for the three nonzero field strengths used in the experiment, normalized with the radius of a field-free ring at the same time (injection height $h=1.27$ cm, dashed curve). For each curve, 90 video frames (sampling rate 30 frames/sec) are analyzed. The trend toward accelerated growth in increasing magnetic fields is clearly visible. These trajectories might eventually be compared to those obtainable by numerical simulation.^{4,5} The advantage of the magnetic strain method compared to, say, surface impingement studies, is the absence of boundaries. Surface tension

effects⁶ which are very difficult to quantify properly, are eliminated in this bulk flow geometry.

The experiments demonstrate the feasibility of creating magnetic vortex rings and the possibility of controlling their evolution through external magnetic fields. It appears that the forced growth of the rings is accompanied by the generation of azimuthal instabilities. In the case of an adverse force field, the rings are destroyed almost immediately. In order to further understand the occurring phenomena, the present measurement technique should be coupled with direct flow velocity measurements. Optical tracer-based techniques such as digital particle imaging velocimetry⁷ should be well suited as they can be incorporated directly into the present digital video acquisition system. A definition seems necessary for the "lifetime" of a vortex ring since the core remnants may be moved by the magnetic field even after the core vorticity has decayed. An extension of the present technique lies in the use of oscillatory or even pulsed magnetic fields. For the investigation of vortex ring instabilities these methods might permit detailed measurements of frequency-selective phenomena or the creation of well-defined, transient deformation states of the vortex rings.

ACKNOWLEDGMENTS

This research was supported in part by DARPA/ACMP URI Grant No. N00014-86-K-0758.

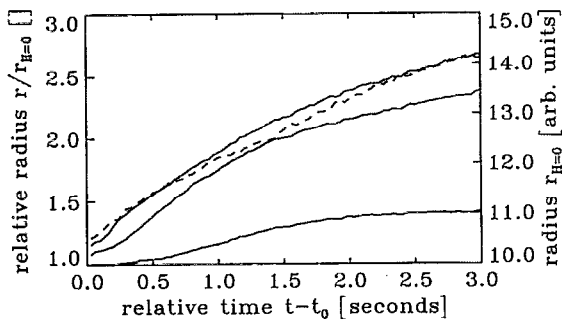


FIG. 5. Normalized ring radii as function of time for different field strengths: $H=14.1, 28.2, 42.3$ kA/m; the reference ring trajectory ($H=0$) is shown as the dashed curve.

^{a)}Present address: European Space Agency ESA/ESTEC, WDS, Postbus 299, NL-2200 AG Noordwijk, Netherlands.

¹R. E. Rosensweig, *Ferrohydrodynamics* (Cambridge U.P., Cambridge, 1985), pp. 112 and 114.

²W. R. Smythe, *Static and Dynamic Electricity*, 2nd ed. (McGraw-Hill, New York, 1950), p. 270.

³EMG 905, Ferrofluidics Corp., Nashua, New Hampshire (saturation magnetization 400 G).

⁴P. Orlandi, "Vortex dipole rebound from a wall," *Phys. Fluids A* **2**, 1429 (1990).

⁵S. Ohring and H. J. Lugt, "Interaction of a viscous vortex pair with a free surface," *J. Fluid Mech.* **227**, 47 (1991).

⁶L. B. Bernal, A. Hirs, J. T. Kwon, and W. W. Wilmarth, "On the interaction of vortex rings and pairs with a free surface for varying amounts of surface active agent," *Phys. Fluids A* **1**, 2001 (1989).

⁷C. E. Willert and M. Gharib, "Digital particle imaging velocimetry," *Exp. Fluids* **10**, 181 (1991).